SPACE SCIENCES

Abundant presolar grains and primordial organics preserved in carbon-rich exogenous clasts in asteroid Ryugu

Ann. N. Nguyen[1]*, Prajkta Mane[2], Lindsay P. Keller[1], Laurette Piani[3], Yoshinari Abe[4], Jérôme Aléon[5], Conel M. O'D. Alexander[6], Sachiko Amari[7,8], Yuri Amelin[9], Ken-ichi Bajo[10], Martin Bizzarro[11], Audrey Bouvier[12], Richard W. Carlson[6], Marc Chaussidon[13], Byeon-Gak Choi[14], Nicolas Dauphas[15], Andrew M. Davis[15], Tommaso Di Rocco[16], Wataru Fujiya[17], Ryota Fukai[18], Ikshu Gautam[19], Makiko K. Haba[19], Yuki Hibiya[20], Hiroshi Hidaka[21], Hisashi Homma[22], Peter Hoppe[23], Gary R. Huss[24], Kiyohiro Ichida[25], Tsuyoshi Iizuka[26], Trevor R. Ireland[27], Akira Ishikawa[19], Shoichi Itoh[28], Noriyuki Kawasaki[10], Noriko T. Kita[29], Kouki Kitajima[29], Thorsten Kleine[30], Shintaro Komatani[25], Alexander N. Krot[24], Ming-Chang Liu[31], Yuki Masuda[19], Kevin D. McKeegan[31], Mayu Morita[25], Kazuko Motomura[32], Frédéric Moynier[13], Izumi Nakai[33], Kazuhide Nagashima[24], David Nesvorný[34], Larry Nittler[6,35], Morihiko Onose[25], Andreas Pack[16], Changkun Park[36], Liping Qin[37], Sara S. Russell[38], Naoya Sakamoto[39], Maria Schönbächler[40], Lauren Tafla[31], Haolan Tang[31], Kentaro Terada[41], Yasuko Terada[42], Tomohiro Usui[17], Sohei Wada[10], Meenakshi Wadhwa[35], Richard J. Walker[43], Katsuyuki Yamashita[44], Qing-Zhu Yin[45], Tetsuya Yokoyama[19], Shigekazu Yoneda[46], Edward D. Young[31], Hiroharu Yui[47], Ai-Cheng Zhang[48], Tomoki Nakamura[49], Hiroshi Naraoka[50], Takaaki Noguchi[28], Ryuji Okazaki[50], Kanako Sakamoto[18], Hikaru Yabuta[51], Masanao Abe[18], Akiko Miyazaki[18], Aiko Nakato[18], Masahiro Nishimura[18], Tatsuaki Okada[18], Toru Yada[18], Kasumi Yogata[18], Satoru Nakazawa[18], Takanao Saiki[18], Satoshi Tanaka[18], Fuyuto Terui[52], Yuichi Tsuda[18], Sei-ichiro Watanabe[21], Makoto Yoshikawa[18], Shogo Tachibana[53], Hisayoshi Yurimoto[10,38]

Preliminary analyses of asteroid Ryugu samples show kinship to aqueously altered CI (Ivuna-type) chondrites, suggesting similar origins. We report identification of C-rich, particularly primitive clasts in Ryugu samples that contain preserved presolar silicate grains and exceptional abundances of presolar SiC and isotopically anomalous organic matter. The high presolar silicate abundance (104 ppm) indicates that the clast escaped extensive alteration. The 5 to 10 times higher abundances of presolar SiC (~235 ppm), N-rich organic matter, organics with N isotopic anomalies (1.2%), and organics with C isotopic anomalies (0.2%) in the primitive clasts compared to bulk Ryugu suggest that the clasts formed in a unique part of the protoplanetary disk enriched in presolar materials. These clasts likely represent previously unsampled outer solar system material that accreted onto Ryugu after aqueous alteration ceased, consistent with Ryugu's rubble pile origin.

INTRODUCTION

The JAXA Hayabusa2 spacecraft collected samples from the C-type asteroid (162173) Ryugu during two touchdown events. The mineralogical, chemical, petrologic, and isotopic characteristics of Ryugu samples have linked them to CI carbonaceous chondrites (1). Ryugu and CI chondrites are chemically primitive but have undergone extensive low-temperature (~30° to 37°C for Ryugu) aqueous alteration that converted most of the initial anhydrous constituents to phyllosilicates, carbonates, magnetite, phosphate, and sulfides (1–4). Anhydrous minerals, like olivine, pyroxene, and spinel, are rare in Ryugu and CI chondrites and mainly exist within Fe-rich clasts (3, 5, 6). The matrix of some of these clasts also contains hydrated phases similar to the major Ryugu lithology (5).

The relative degree of parent body alteration across different samples and lithologies can be gauged through analysis of nanometer- to micrometer-sized presolar grains, found as trace components in chondrites, interplanetary dust particles (IDPs), Antarctic micrometeorites (AMMs), and comet 81P/Wild 2 samples returned by NASA's Stardust mission (7). Presolar grains condensed in the outflows and ejecta of dying stars, such as red giants, supernovae, and novae, and retain the highly anomalous isotopic signatures of their parent stars (7). The isotopic compositions of presolar grains are diagnostic of the evolution and nucleosynthetic reactions that occurred within their stellar sources. Identified presolar phases include nanodiamonds, carbides, graphite, silicon nitride, oxides, and silicates (7, 8). These phases are affected by secondary processes to varying degrees, and hence, their relative abundances in extraterrestrial materials, microstructures, and chemistry convey the extent of parent body hydrothermal alteration [e.g., (9, 10, 11)].

Primitive extraterrestrial samples also contain large H and N isotopic anomalies carried by insoluble organic matter (IOM) (12–15). The D and ^{15}N enrichments likely result from low-temperature chemical reactions in either the cold presolar molecular cloud or outer protosolar disk (16, 17). More rarely, IOM bearing moderate C isotopic anomalies has been observed (18–20). Parent body

processing appears to decrease or destroy isotopic anomalies, particularly those in H, in IOM, but the effects are complicated and poorly understood (15). To investigate Ryugu's origin, history, and extent of aqueous alteration and thermal metamorphism, we determined the abundances and isotopic, chemical, and mineralogical characteristics of presolar grains and isotopically anomalous organic matter (IAOM) within various lithologies.

RESULTS

The elemental compositions of fragments of Ryugu particles C0002 and A0040 were determined by field-emission scanning electron microscopy and energy-dispersive x-ray spectroscopy (FE-SEM-EDX), revealing a phyllosilicate-dominated CI-like matrix enclosing S- and Fe-rich and Mg- and Si-poor clasts. These clasts were present as discrete regions having well-defined boundaries with the hydrated matrix (clasts 1 to 3, ~50 to 100 μm in size) (Figs. 1 and 2 and figs. S1 and S3) and as more diffuse regions where the boundaries between the clast and host matrix were less clear (clasts 4 and 5, ~50 to 200 μm in size) (fig. S2). The matrix of chondritic samples is the fine-grained groundmass between more coarse objects such as chondrules. It consists predominantly of silicates that may be crystalline, amorphous, anhydrous, or hydrated, and it also contains organic matter. It is within this matrix that most presolar grains are found. Presolar grains and IAOM were identified in interclast matrix and five clasts (e.g., Fig. 2 and figs. S3 and S4) by C, N, O, and Si isotopic mapping using nanoscale secondary ion mass spectrometry (NanoSIMS).

A total of 58 C-rich presolar grains were identified. Fifty grains were ^{13}C-rich, and 8 were ^{13}C-poor (fig. S5 and table S1). Most of these grains likely condensed around solar to lower-than-solar metallicity asymptotic giant branch (AGB) stars, and some grains have supernova signatures (7). On the basis of the NanoSIMS ^{28}Si$^-$/^{12}C$^-$ ratios, 47 of the grains were silicon carbide (SiC) and 11 were graphite. The mineralogical and chemical characterization of ^{13}C-rich grain C0002-C11 (table S1) from clast 1 by scanning transmission electron microscopy (STEM) indicated a polycrystalline SiC with multiple 20- to 50-nm–sized subgrains, some of which showed unit cell–scale twinning (fig. S6). The structure was consistent with cubic 3C β-SiC, the most common polytype. This grain had a partially oxidized rim likely resulting from secondary alteration.

Clast 1 in C0002 (Fig. 1) also contained two highly ^{17}O-rich grains of likely AGB star origin and one ^{18}O-rich supernova grain (Fig. 2, figs. S3 and S5, and table S1). STEM analysis of ^{17}O-rich grain C0002-C3 in clast 1 confirmed that it is a Mg-, Fe-, and Al-bearing silicate (Fig. 3) with pyroxene stoichiometry [$(Mg_{0.8}Fe_{0.2})(Si, Al)O_3$]. Diffraction data from the grain showed diffuse scattering, consistent with an amorphous structure. The stoichiometric chemical composition suggests that the grain condensed as a crystal in the parent circumstellar environment and was later amorphized, likely by irradiation in space. Presolar grains C0002-C1 and C0002-C2 had NanoSIMS ^{28}Si$^-$/^{16}O$^-$ and ^{24}Mg^{16}O$^-$/^{16}O$^-$ ratios similar to C0002-C3 (table S1), implying that they are also silicates.

The abundances of presolar grains in the different analyzed clasts and matrix regions are given in table S2 and shown in fig. S7. The presolar silicate abundance in clast 1 is 104^{+102}_{-57} parts per million (ppm) (1σ), and the upper abundances in the other lithologies are <18 ppm. Clasts 1 and 2 have similarly high abundances of presolar SiC, 277^{+127}_{-91} and 219^{+70}_{-54} ppm, respectively, whereas the other analyzed lithologies had abundances <73 ppm. Presolar graphite abundances for all analyzed lithologies were <38 ppm.

A total of 433, mainly submicrometer-sized grains showed N isotopic anomalies and low ^{28}Si$^-$/^{12}C$^-$ ratios, suggestive of organic matter (table S3, Fig. 4, and fig. S8). Both ^{15}N enrichments (δ^{15}N ~ +200 to +3200‰) and depletions (δ^{15}N ~ −170 to −500‰)

[1]Astromaterials Research and Exploration Science, NASA Johnson Space Center, Houston, TX 77058, USA. [2]Universities Space Research Association, Lunar and Planetary Institute, Houston, TX 77058, USA. [3]Centre de Recherches Pétrographiques et Géochimiques, CNRS - Université de Lorraine, Nancy 54500, France. [4]Graduate School of Engineering Materials Science and Engineering, Tokyo Denki University, Tokyo 120-8551, Japan. [5]Institut de Minéralogie, de Physique des Matériaux et de Cosmochimie, Sorbonne Université, Museum National d'Histoire Naturelle, CNRS UMR 7590, IRD, Paris 75005, France. [6]Earth and Planets Laboratory, Carnegie Institution for Science, Washington, DC 20015, USA. [7]McDonnell Center for the Space Sciences and Physics Department, Washington University, St. Louis, MO 63130, USA. [8]Geochemical Research Center, The University of Tokyo, Tokyo 113-0033, Japan. [9]Guangzhou Institute of Geochemistry, Chinese Academy of Sciences, Guangzhou, GD 510640, China. [10]Department of Natural History Sciences, IIL, Hokkaido University, Sapporo 001-0021, Japan. [11]Centre for Star and Planet Formation, GLOBE Institute, University of Copenhagen, Copenhagen K 1350, Denmark. [12]Bayerisches Geoinstitut, Universität Bayreuth, Bayreuth 95447, Germany. [13]Université Paris Cités, Institut de physique du globe de Paris, CNRS, Paris 75005, France. [14]Department of Earth Science Education, Seoul National University, Seoul 08826, Republic of Korea. [15]Department of the Geophysical Sciences and Enrico Fermi Institute, The University of Chicago, 5734 South Ellis Avenue, Chicago, IL 60637, USA. [16]Faculty of Geosciences and Geography, University of Göttingen, Göttingen D-37077, Germany. [17]Faculty of Science, Ibaraki University, Mito 310-8512, Japan. [18]Institute of Space and Astronautical Science, Japan Aerospace Exploration Agency, Sagamihara 252-5210, Japan. [19]Department of Earth and Planetary Sciences, Tokyo Institute of Technology, Tokyo 152-8551, Japan. [20]General Systems Studies, The University of Tokyo, Tokyo 153-0041, Japan. [21]Earth and Planetary Sciences, Nagoya University, Nagoya 464-8601, Japan. [22]Osaka Application Laboratory, SBUWDX, Rigaku Corporation, Osaka 569-1146, Japan. [23]Max Planck Institute for Chemistry, Mainz 55128, Germany. [24]Hawai'i Institute of Geophysics and Planetology, University of Hawai'i at Mānoa, Honolulu, HI 96822, USA. [25]Analytical Technology, Horiba Techno Service Co. Ltd., Kyoto 601-8125, Japan. [26]Earth and Planetary Science, The University of Tokyo, Tokyo 113-0033, Japan. [27]School of Earth and Environmental Sciences, The University of Queensland, St. Lucia, QLD 4072, Australia. [28]Earth and Planetary Sciences, Kyoto University, Kyoto 606-8502, Japan. [29]Department of Geoscience, University of Wisconsin-Madison, Madison, WI 53706, USA. [30]Max Planck Institute for Solar System Research, Göttingen 37077, Germany. [31]Earth, Planetary, and Space Sciences, UCLA, Los Angeles, CA 90095, USA. [32]Thermal Analysis, Rigaku Corporation, Tokyo 196-8666, Japan. [33]Applied Chemistry, Tokyo University of Science, Tokyo 162-8601, Japan. [34]Department of Space Studies, Southwest Research Institute, Boulder, CO 80302, USA. [35]School of Earth and Space Exploration, Arizona State University, Tempe, AZ 85281, USA. [36]Earth System Sciences, Korea Polar Research Institute, Incheon 21990, Korea. [37]CAS Key Laboratory of Crust-Mantle Materials and Environments, University of Science and Technology of China, School of Earth and Space Sciences, Anhui 230026, China. [38]Department of Earth Sciences, Natural History Museum, London SW7 5BD, UK. [39]Isotope Imaging Laboratory, Creative Research Institution, Hokkaido University, Sapporo 001-0021, Japan. [40]Institute for Geochemistry and Petrology, Department of Earth Sciences, ETH Zurich, Zurich, Switzerland. [41]Earth and Space Science, Osaka University, Osaka 560-0043, Japan. [42]Spectroscopy and Imaging, Japan Synchrotron Radiation Research Institute, Hyogo 679-5198, Japan. [43]Department of Geology, University of Maryland, College Park, MD 20742, USA. [44]Graduate School of Natural Science and Technology, Okayama University, Okayama 700-8530, Japan. [45]Earth and Planetary Sciences, University of California, Davis, Davis, CA 95616, USA. [46]Science and Engineering, National Museum of Nature and Science, Tsukuba 305-0005, Japan. [47]Department of Chemistry, Tokyo University of Science, Tokyo 162-8601, Japan. [48]School of Earth Sciences and Engineering, Nanjing University, Nanjing 210023, China. [49]Department of Earth Science, Tohoku University, Sendai 980-8578, Japan. [50]Department of Earth and Planetary Sciences, Kyushu University, Fukuoka 819-0395, Japan. [51]Earth and Planetary Systems Science Program, Hiroshima University, Higashi-Hiroshima 739-8526, Japan. [52]Kanagawa Institute of Technology, Atsugi 243-0292, Japan. [53]UTokyo Organization for Planetary and Space Science, University of Tokyo, Tokyo 113-0033, Japan.
*Corresponding author. Email: Ian-anh.n.nguyen@nasa.gov
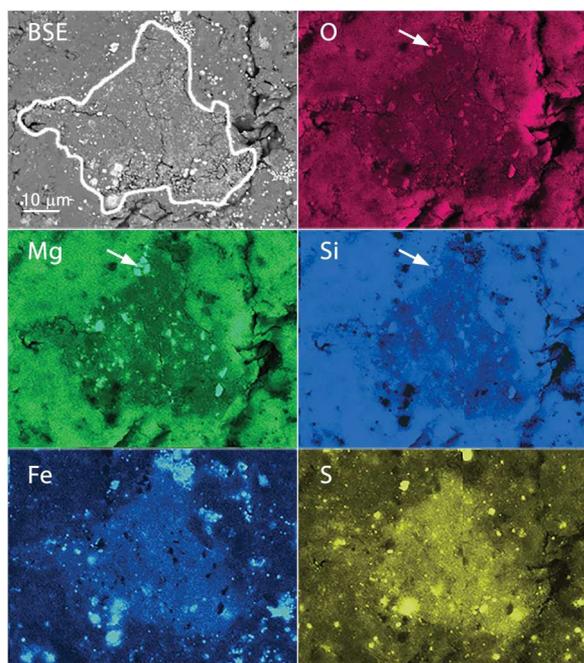
Fig. 1. Backscattered electron (BSE) image and elemental maps of a region of grain C0002 containing primitive clast 1, outlined in the BSE image. This clast is rich in Fe and S and depleted in Mg, Si, and O compared to the surrounding matrix. It also contains Mg-rich silicate grains that are likely olivine. White arrows indicate a cluster of these grains.

were observed. Eleven percent of these grains had moderate C isotopic anomalies (δ^{13}C ranging from ±250‰). Of the grains having C isotopic anomalies, 60% were enriched in ^{15}N. Three grains had anomalous C isotopic compositions and isotopically normal N compositions. The range of N and C isotopic compositions associated with organic matter was similar among the Ryugu lithologies. We analyzed one grain from clast 1 having 220 and 240‰ depletions in ^{13}C and ^{15}N, respectively, by TEM (fig. S9). The 300-nm–sized amorphous grain contained C, N, O, and S, likely associated with N-based and carbonyl (C=O) functionality and an organo-S component, confirming that the grain is organic and not graphitic. These results imply that other grains having moderately anomalous C isotopic compositions and low ^{28}Si$^-$/^{12}C$^-$ ratios are also organic.

DISCUSSION
Distribution of presolar grains
Presolar silicate grains are rapidly destroyed by aqueous alteration and are only preserved in very primitive samples (*9*). For example, presolar silicates have yet to be identified in the highly aqueously altered CI chondrites, and the highest reported abundances occur in anhydrous IDPs that are believed to have cometary origins [e.g., (*21*)]. We identified presolar silicates only in C0002 clast 1 at an abundance of 104^{+102}_{-57} ppm (1σ; Fig. 5 and table S2). In another study of Ryugu, a clast less-altered than bulk Ryugu had a presolar silicate abundance of 25^{+33}_{-16} ppm (*22*). For the Ryugu matrix and clasts 3 to 5, we determined a 1σ upper abundance limit for presolar O-rich grains of 3 ppm. This upper limit is consistent with abundances in another study of Ryugu [5^{+5}_{-3} ppm; (*22*)],

the upper limit for the CI chondrite Ivuna [4 ppm; (*22*)], and aqueously altered samples of all chondrite classes (*9*). More than 50% of the Ryugu matrix is composed of phyllosilicates (*2*), and the aqueous alteration that produced the hydrated matrix very likely destroyed presolar silicate grains.

The preservation of presolar silicates in clast 1 indicates that it is less altered than the host Ryugu matrix, in agreement with our TEM observations showing that clast 1 is dominated by amorphous silicates and GEMS (glass with embedded metal and sulfide)–like grains, with minor phyllosilicates, sulfides, rare magnetite, C nanoglobules, and forsterite (fig. S10). These constituents resemble those in the least altered fragments found by (*3*) in Ryugu. The matrix of clast 1 is most similar to the matrices of weakly altered CR2 (Renazzo-type) chondrites [e.g., QUE 99177, MET 00426; (*23*, *24*)]. The presolar silicate abundance in clast 1 is comparable to those in less altered CRs, CO3s (Ornans-type), and ungrouped chondrites (*9*) but is also within error of the highest reported abundance in chondrite matrices (~240 ± 30 ppm in CO3 DOM 08006) (Fig. 5) (*19*, *25*). The range of abundances observed in chondrite matrices is attributed to parent body aqueous alteration. While all asteroids experienced some degree of parent body alteration, comets remain largely unaltered since their formation in the cold outer solar system. The abundance of presolar silicates in comet Wild 2 samples was estimated to be 600 to 830 ppm (*26*). Anhydrous IDPs and some AMMs have characteristics that suggest cometary origins. Reported presolar silicate abundances in anhydrous IDPs vary widely, ranging from 140^{+320}_{-120} ppm (*27*) to $15,000^{+8170}_{-5590}$ ppm (*21*). A subset of IDPs proposed to be "isotopically primitive" has an average abundance of 375 ppm (*28*), and the area-weighted average for all measured anhydrous IDPs is 400 ppm (*29*). A similar abundance of 360^{+200}_{-130} ppm was determined for a C-rich cometary clast found in the CR2 chondrite LAP 02342 (*30*). The highest abundance reported for AMMs is 170^{+58}_{-45} ppm (*31*). The abundance of presolar silicates in clast 1 is lower than that of comet Wild 2 but is consistent with abundances in some AMMs and IDPs of probable cometary origin.

Unlike presolar silicates, presolar SiC and graphite grains survive aqueous alteration but are destroyed by thermal metamorphism or prolonged oxidation (*10*, *32*, *33*). Their abundances are relatively consistent across unheated chondrite classes and types: ~30 ppm for presolar SiC and <10 ppm for presolar graphite (*10*, *32*, *33*). A presolar graphite abundance has not been reported for comet Wild 2, but the presolar SiC abundance was inferred to be 45 ppm (*26*), consistent with chondrites. Only four presolar SiC have been identified in anhydrous IDPs, and estimated abundances range from 60 to 190 ppm (*27*, *34*, *35*). The average presolar SiC abundance in AMMs is 14^{+11}_{-7} ppm (*31*). Presolar graphite grains have not been identified in IDPs and AMMs. No presolar SiC or graphite was found in the C-rich cometary clast (*30*). We found clasts 1 and 2 to have exceptional presolar SiC abundances, 277^{+127}_{-91} ppm (9 grains) and 219^{+70}_{-54} ppm (16 grains), respectively, whereas the other Ryugu lithologies have abundances <73 ppm (table S2 and fig. S7). The combined presolar SiC abundance of 45^{+12}_{-10} ppm in Ryugu, excluding clasts 1 and 2, is consistent with abundances in many unheated chondrites (Fig. 5) (*10*). The presolar graphite abundances across Ryugu lithologies are more consistent, and the average of 12^{+6}_{-4} ppm agrees with the ~10-ppm abundance in CI chondrites Orgueil and Ivuna (*22*, *33*). The similar presolar SiC
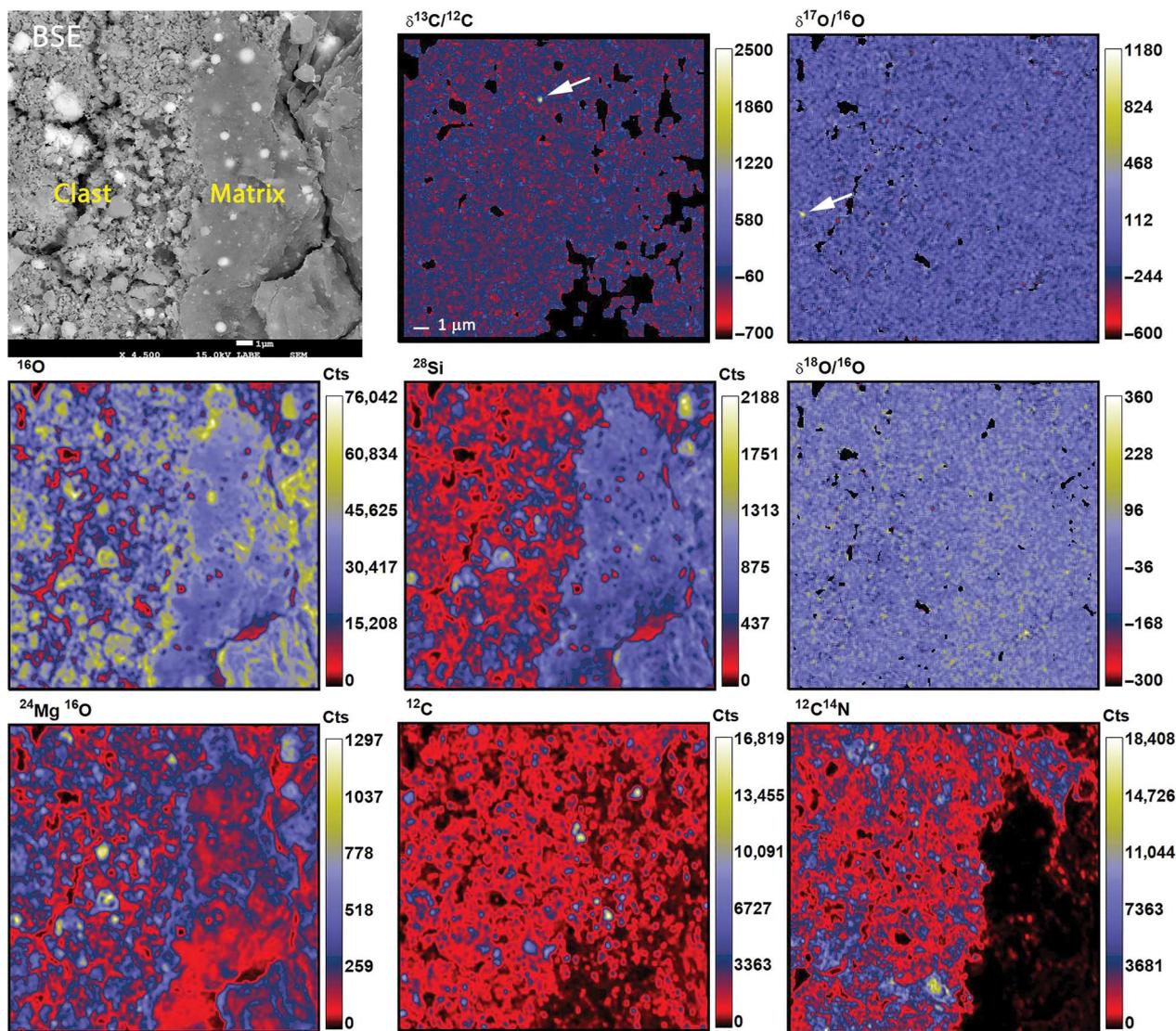
Fig. 2. Region of grain C0002 containing a portion of primitive clast 1 and hydrated Ryugu matrix. The BSE (top left) and corresponding NanoSIMS ^{16}O, ^{28}Si, ^{24}Mg^{16}O, ^{12}C, and ^{12}C^{14}N ion images show that the clast 1 matrix is more fine-grained and has a well-defined boundary with the altered Ryugu matrix. The NanoSIMS ion images show that the clast has lower ^{28}Si signal and greater ^{12}C and ^{12}C^{14}N signals relative to the neighboring matrix, indicative of a higher abundance of N-rich organic matter in the clast. The ^{12}C^{14}N image was acquired in a subsequent measurement, and the analysis region is shifted up by 3 μm relative to the other images. This portion of clast 1 contains ^{17}O-rich presolar silicate C0002-C1 and ^{13}C-rich presolar SiC grain C0002-C7, shown by the arrows in the NanoSIMS δ^{17}O/^{16}O and δ^{13}C/^{12}C ratio images. Isotope ratios are given as deviations from the standard values in per mil (‰). Small variations in the isotope ratio images are due to statistical fluctuations.

and graphite abundances in Ryugu (excluding clasts 1 and 2) and CI and unheated chondrites indicate that the Ryugu samples escaped thermal metamorphism and prolonged oxidation. This agrees with analyses of water in phyllosilicates in Ryugu samples that indicate that Ryugu was never heated above 100°C (*1*). The Ryugu matrix, therefore, accreted in a region of the protoplanetary disk that had an abundance of presolar grains typically observed in chondritic meteorite matrices.

The much higher presolar SiC abundances in clasts 1 and 2, however, indicate that they accreted in a reservoir that was distinct from Ryugu, comet Wild 2, and most chondrites, AMMs, and IDPs. Elevated presolar SiC abundances have only been reported for two CR2 chondrites: 160 ± 57 ppm in NWA 852 and 182 ± 34 ppm

(120^{+28}_{-23} ppm excluding a large grain) in GRV 021710 (Fig. 5) (*36*, *37*). These abundances are similar to those in some anhydrous IDPs. Relative to chondritic meteorites, some IDPs and AMMs show elevated abundances of O-rich supernova stardust having large enrichments in ^{18}O [e.g., (*21*, *31*)], suggesting a heterogeneous distribution of supernova dust in the protoplanetary disk. Most of the presolar SiC grains in clasts 1 and 2 derive from C-rich AGB stars and have C, N, and Si isotopic compositions falling within the mainstream-, Y-, and Z-type classifications for SiC from AGB stars (fig. S5) (*7*). Differences in nucleosynthetic isotopic anomalies in noncarbonaceous and carbonaceous reservoirs have been linked to the heterogeneous distribution of presolar grains in the solar protoplanetary disk (*38*). The observed nucleosynthetic signatures
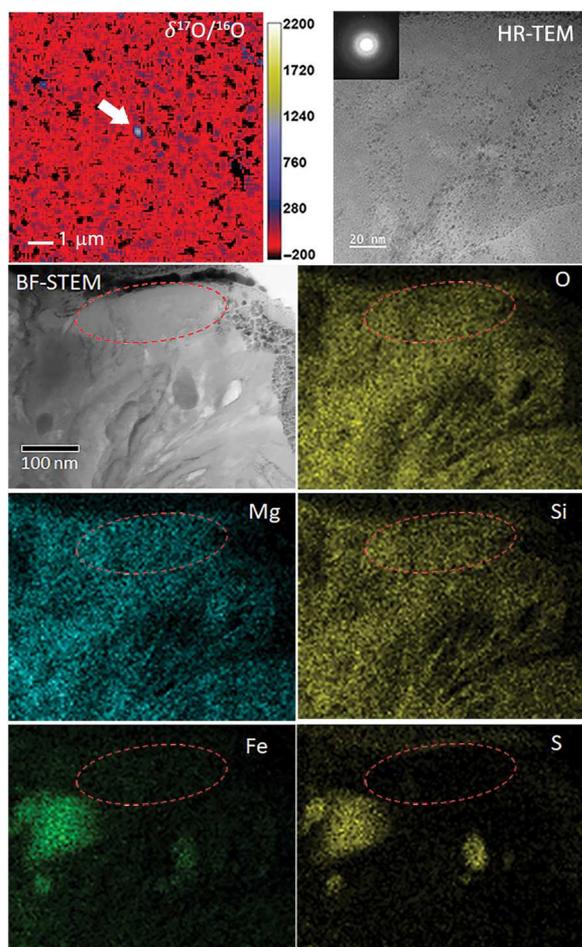
Fig. 3. NanoSIMS and TEM data for the ^{17}O-rich presolar grain C0002-C3. The presolar grain is indicated by the arrow in the ^{17}O/^{16}O ratio image of a region of clast 1 (top left). Isotopic ratios are given as deviations from terrestrial composition in per mil (‰). The inset in the high-resolution TEM (HR-TEM) image shows diffuse scattering consistent with an amorphous structure. The bright-field STEM (BF-STEM) image and elemental maps of the presolar grain (outlined in red) show that it is a silicate with pyroxene stoichiometry and composition $(Mg_{0.8}Fe_{0.2})(Si, Al)O_3$.

require dust contributions from both supernova and AGB stars (*38, 39*). The inventory of refractory presolar grains in IDPs, AMMs, and clasts 1 and 2 in Ryugu samples also points to heterogeneous distributions of stardust from multiple stellar sources in the early solar system.

While we did not find any presolar oxide grains in our study, (*22*) found one grain in the Ryugu matrix for an abundance of 0.6 ppm. From our study, the presolar SiC abundance in the primitive clasts is ~5.5 times greater than in the Ryugu matrix. If presolar oxides are enriched to the same degree in the clasts, then the abundance would be 3.2 ppm. Given the measured area of the clasts and using the average presolar oxide size of 250 nm, we would expect to find <0.3 presolar oxides in each clast. The probability of finding a presolar oxide can also be calculated using the equation $(1 - e^{-A/B}) \times 100$ (%), where A is the area analyzed in each clast and B is the area analyzed by (*22*) to find one grain divided by 5.5 to represent the enhanced abundance in the clasts. The probabilities of finding a

presolar oxide in clasts 1 and 2 are 21 and 50%, respectively. Therefore, our results are not inconsistent with an enrichment in presolar oxides relative to the Ryugu hydrated matrix.

Isotopically anomalous organic matter

Clasts 1 and 2 show greater abundances of organic matter than bulk Ryugu based on the ~5 times higher NanoSIMS $^{12}C^{14}N/^{28}Si$ ratios. This is similar to C-rich anhydrous IDPs and ultracarbonaceous AMMs (UCAMMs) that have C contents >2 × CI (*40, 41*) and the cometary clast found in LAP 02342 (*30*). Clasts 1 and 2 also contain higher abundances of IAOM with N isotopic anomalies, 1.4 and 1.1%, respectively, compared to 0.07 and 0.3% in the C0002 and A0040 matrix, respectively (Fig. 4). Only a few anhydrous IDPs (*34*) and the CR2 chondrite EET 92042 (*13*) show percent level or higher abundances of IAOM. The high C and N contents of clasts 1 and 2 relative to the Ryugu matrix can be seen in the NanoSIMS isotope maps (Fig. 2 and fig. S3). The average NanoSIMS $^{12}C^{14}N/^{12}C$ ratios of IAOM in clasts 1 and 2 are 1.0 and 0.6, respectively, while in the matrix of C0002 and A0040, they are 0.3 and 0.5, respectively. The correlation between the abundance of N isotopic anomalies and $^{12}C^{14}N/^{12}C$ ratio suggests that the N anomalies are mainly carried by N-rich organic matter. IAOM in some anhydrous IDPs is also strongly N-rich (*14*). The bulk $^{12}C^{14}N/^{12}C$ ratios for the clasts and matrix are similar to the average ratios of the respective IAOM. Therefore, the organic matter in the clasts is intrinsically about two times more N-rich than organic matter in the Ryugu matrix. Organic matter in comet Wild 2 and some UCAMMs have higher N contents than chondrites and IDPs (*41, 42*). It has been proposed that the organic matter in the UCAMMs formed by chemical reactions of N- and methane-rich ices beyond the trans-Neptunian region of the solar system (*41*). The organic matter in the clasts likely also formed in the outer solar system.

We found clasts 1 and 2 to have remarkably high abundances of IAOM having C isotopic anomalies—0.3 and 0.2%, respectively—compared to 0.02% in the Ryugu matrix. Such rare C-anomalous organic grains have only been identified in three CR2 chondrites (*13, 18, 43*) and some anhydrous IDPs (*12, 20, 28, 44*). Their abundance in the minimally altered CR2 chondrites QUE 99177 and MET 00426 (~0.012%) led (*18*) to suggest that aqueous alteration destroys the carriers of the C isotopic anomalies. However, the hydrated Ryugu matrix contains a similar abundance of C-anomalous IAOM as the CR2 chondrites, and the overall abundance of IAOM with N anomalies (0.17%) in the Ryugu matrix is comparable to chondritic IOM [0.005 to 1%; (*13*)] and anhydrous IDPs [0.08%; (*28*)]. The range of N isotopic ratios in the Ryugu IAOM also rivals those in primitive chondrites (*13, 18, 43*), anhydrous IDPs (*21, 28, 44*), C-rich AMMs (*41*), and comet Wild 2 (*45, 46*), with the most extreme isotopic hotspot in hydrated Ryugu ($\delta^{15}N \sim 3200$‰) exceeding those in pristine samples. These observations suggest that aqueous alteration does not erase or dilute the N and C isotopic signatures of IAOM, similar to previous studies of chondritic IOM residues [e.g., (*47*)]. The similar abundances and compositions of IAOM suggest that the parent bodies of Ryugu and some CR chondrites and anhydrous IDPs accreted common primordial organic matter.

That the organic matter in clasts 1 and 2 shows higher N contents, higher abundances of N isotopic anomalies, and the highest abundance of C-anomalous IAOM ever reported implies that the accreted IAOM formed in a region of the cold molecular cloud
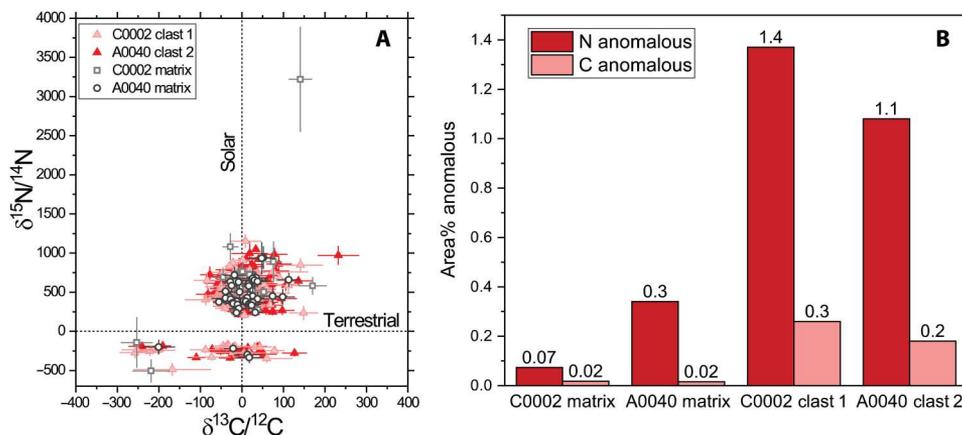
Fig. 4. Isotopic compositions and abundances of IAOM in the Ryugu matrix and primitive clasts 1 and 2. The IAOM in the different lithologies has similar C and N isotopic distributions (**A**). However, the clasts have much higher abundances of IAOM [%; (**B**)] than the Ryugu matrix. Isotopically normal organic matter is not plotted. Errors in (A) are 1σ.
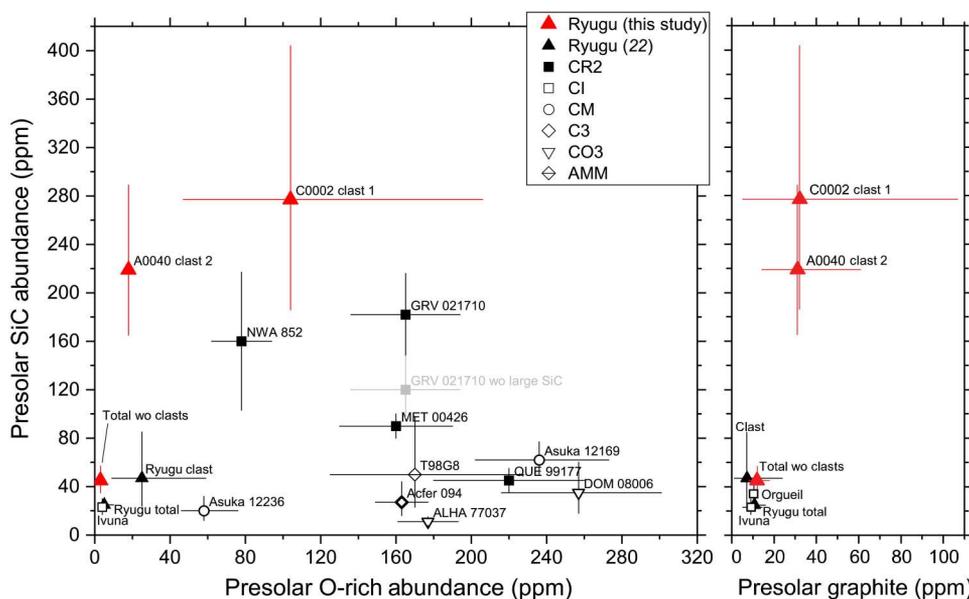
Fig. 5. Abundances of presolar grains in Ryugu, carbonaceous chondrites, and an AMM. Abundances of presolar silicates and oxides (O-rich), SiC, and graphite in clasts 1 and 2 and Ryugu matrix compared to abundances in chondrites of various classes [(9) and references therein (10, 18, 19, 22, 33, 36, 37, 51)] and an AMM (31). The abundances in Ryugu are consistent with CI chondrites except for clasts 1 and 2, which have remarkably high abundances of presolar SiC grains. The presolar silicate abundance in clast 1 is similar to primitive chondrites and not altered CI. Presolar O-rich grain abundances for A0040 clast 2, total Ryugu without clasts, and Ivuna (22) are upper limits. Errors are 1σ. wo, without. Not plotted are presolar grain abundances in comet Wild 2 and IDPs. The abundance of O-rich presolar grains in comet Wild 2 samples is 600 to 830 ppm, and the abundance of presolar SiC is 45 ppm (26). Anhydrous IDPs display a wide range of presolar abundances for O-rich grains (20 to 23,080 ppm including 1σ errors) and SiC grains (10 to 630 ppm including 1σ errors) (21, 27, 34, 35).

distinct from the formation region of IAOM in bulk Ryugu and known chondritic materials. Theoretical models of gas-phase ion-molecule reactions in dense interstellar clouds reproduce the C and N isotopic compositions of IAOM in chondrites, IDPs, and Ryugu samples, with the isotopic anomalies produced in specific molecules (17, 48–50). While the abundances of N-bearing molecules do not vary with gas density, the abundances of the C-bearing molecules are generally greater at lower densities and when C/O > 1 (49). The IAOM in clasts 1 and 2 likely formed where the physical and chemical conditions were favorable for C isotopic fractionation, and

the resulting anomalies escaped equilibration with isotopically normal CO. The paucity of C-anomalous IAOM in chondritic meteorites and IDPs suggests that the chemical reactions that fractionate N were more efficient or widespread than those that fractionate C (49), the molecules in which C fractionates were depleted in the environment where most IAOM formed, the conditions were not conducive to C isotopic fractionation (50), and/or equilibration was prevalent.

Our studies of grain A0040 collected during the first touchdown of the Hayabusa2 spacecraft and grain C0002 collected during the

second touchdown revealed a difference in the organic matter. Although the abundance of IAOM with C isotopic anomalies were the same in the hydrated matrices of C0002 and A0040, the abundance of N anomalous IAOM was greater in the A0040 matrix. The average $^{12}C^{14}N/^{12}C$ ratios of both the isotopically normal organic matter and IAOM in A0040 are two times the ratios in C0002. This indicates that the organic matter in the matrix of A0040 was more N-rich than the matrix of C0002, though not as N-rich as the primitive clasts. These differences likely reflect inherent heterogeneity of organic matter in Ryugu rather than alteration during potential exposure of A0040 on the surface of Ryugu. Processes that fractionate N would also be expected to fractionate C and the matrices of A0040 and C0002 had the same abundance of C anomalous IAOM.

Origin of clasts in Ryugu samples

The uniquely primitive characteristics of clasts 1 and 2 set them apart from the bulk of the Ryugu matrix and any other known extraterrestrial materials. These clasts have (i) moderate abundance of preserved presolar silicate grains, (ii) primitive mineralogy, (iii) abundances of presolar SiC exceeding any other sample, (iv) high abundances of organic matter with N isotopic anomalies, (v) abundances of organic matter with C isotopic anomalies exceeding any other sample, and (vi) very high abundances of N-rich organic matter. While some CR chondrites and chondritic IDPs have presolar SiC or IAOM abundances approaching those in these clasts, no sample has similarly high abundances of both constituents. Moreover, the abundance of C-anomalous IAOM in clasts 1 and 2 is unparalleled.

The abundance of presolar silicates and the mineralogy of clast 1 indicate that it experienced limited aqueous alteration, unlike bulk Ryugu. However, the other characteristics of clasts 1 and 2 cannot be explained by more limited aqueous alteration relative to the host Ryugu matrix. Presolar SiC is not altered or destroyed by aqueous alteration. This is exemplified by the similar abundances of these grains in hydrated and less altered chondrites (10), AMMs (31), an anhydrous IDP (35), and comet Wild 2 (26). The abundance of presolar SiC in the Ryugu matrix is comparable to these samples. Therefore, parent body aqueous alteration cannot explain the lower abundance of presolar SiC in the Ryugu matrix compared to the clasts. The similar C and N isotopic distributions of organic matter in the clasts and Ryugu matrix indicate that the molecular carriers of these anomalies are not destroyed and the isotopic anomalies are not diluted by aqueous alteration. Previous studies of chondrites have also shown that aqueously altered samples have similar N isotopic anomalies and abundances of IAOM as less altered samples, including primitive anhydrous IDPs and comet Wild 2 (see discussion above). Thus, the lower abundance of IAOM in the Ryugu matrix is not attributable to aqueous alteration. The lower abundance of organic matter in the Ryugu matrix relative to the clasts also cannot be explained by aqueous alteration. Altered CI chondrites have greater abundances of C associated with organic matter than more primitive chondrites [e.g., (47)].

Clasts 1 and 2 may therefore represent a previously unsampled type of primitive chondritic material that accreted in a cold region of the protoplanetary disk enriched in presolar grains and primordial organics. We propose that these unique clasts are exogenous and originated from an asteroid or comet in the outer solar system. The bulk δD and δ^{15}N compositions (4), observation of CO_2-bearing water inclusions within pyrrhotite (3), and N/C ratios of Ryugu samples (3) indicate that Ryugu also likely formed in the outer solar system, similar to CI chondrites. Probable cometary samples have higher C abundances than CI chondrites and N-rich organic matter. The significantly greater abundance of organic matter in the clasts and its N-rich nature compared to bulk CI-like Ryugu support a cometary origin. In addition, the presolar silicate abundance in clast 1 is consistent with some anhydrous IDPs and AMMs. The clasts have clearly escaped the extensive hydration experienced by the Ryugu matrix and have distinct boundaries with the Ryugu matrix. It is therefore less likely that they were incorporated during accretion of the matrix material of Ryugu's parent asteroid. Instead, the clasts most likely accreted onto Ryugu >5 million years after solar system formation, when aqueous alteration ceased on Ryugu's progenitor body (1) and after the parent body was disrupted to form Ryugu as a rubble pile at large radial distance (2).

While the other clasts studied here are chemically similar to clasts 1 and 2, they differ substantially in their inventory of presolar grains and IAOM and are indistinguishable from bulk Ryugu in that regard. These clasts likely have a different origin from clasts 1 and 2. Whereas clasts 1 and 2 have well-defined boundaries with the Ryugu matrix, the diffuse nature of clasts 4 and 5 suggests that they were part of the progenitor Ryugu planetesimal. Their chemical resemblance to primitive clasts 1 and 2 indicates that they were not as extensively altered as the surrounding Ryugu matrix. These nanometer-scale coordinated analyses of Ryugu returned samples have provided incredibly detailed insights into the macroscale accretion and alteration processes that occurred on the Ryugu asteroid and parent body, and the distribution of presolar grains and IAOM in the protoplanetary disk. The preservation of abundant primitive materials within a highly altered body cannot be observed remotely and emphasizes the importance of laboratory analyses of returned samples.

MATERIALS AND METHODS
Experimental design
The objective of the study was to characterize the presolar grains and IAOM within various lithologies present in Ryugu samples. This was done by conducting coordinated nanoscale isotopic, chemical, and mineralogical analyses of isotopically anomalous components and their host matrix. Samples were examined by FE-SEM-EDX, NanoSIMS, and TEM assisted by focused ion beam (FIB) sample preparation techniques.

Samples and preparation
Broken fragments from Ryugu grains from the first touchdown site (A0040 from chamber A) and second touchdown site (C0002 from chamber C) were examined in this study. The fragments were submillimeter sized. The fragments were handpicked and pressed into pure indium in two separate sample mounts. The samples were not polished because of their highly friable nature and also to avoid contamination and/or removal of soluble organic compounds by exposure to solvents. Polished grains of San Carlos olivine and Madagascar hibonite were also pressed into each mount and served as reference materials. Additional isotopic carbonate and amphibole standards were included in the mounts but not used in this study. One fragment from C0002 and three fragments

from A0040 were studied. The samples were coated with ~5 nm of Pt using a Cressington 108 auto sputter coater for SEM and Nano-SIMS analyses.

FE-SEM-EDX chemical analysis
Fragments of Ryugu grains C0002 and A0040 were first imaged and characterized for their elemental compositions by FE-SEM-EDX. The JEOL 7600F at NASA Johnson Space Center (JSC) was used to capture ultrahigh spatial resolution (2 to 3 nm) secondary electron images (SEIs), and backscattered electron images (BEIs) of the samples. The SEIs were used to identify flat regions of the sample that would be appropriate for NanoSIMS isotopic analysis. Detailed images of these regions were acquired along with elemental x-ray maps of Ti, Si, S, P, O, Ni, Na, Mg, K, In, Fe, Cr, Cl, Ca, C, and Al. The JEOL 7600F is equipped with a silicon drift detector (SDD)–type x-ray detector system, which can acquire and process >100,000 x-ray counts per second.

Among a phyllosilicate-dominated groundmass were magnetite framboids, plaquettes and spherules, carbonates, sulfides, Al-rich and Fe-rich oxides, chromite, Mg-rich silicates, and carbonaceous veins, nodules, and globules. The BEI and elemental maps allowed for detection of clasts, which appeared lighter in the BEI and chemically distinct from surrounding matrix. These clasts were irregularly shaped and existed as discrete regions <100 μm in size and as more diffuse regions. They were relatively Fe- and S-rich and Mg- and Si-poor compared to the surrounding Ryugu matrix. Clast 1 was also Ni-rich and Na-poor and contained <~2-μm–sized Mg-rich silicates, likely olivine.

NanoSIMS isotopic analysis
Isotopic analysis of the Ryugu samples was conducted using the CAMECA NanoSIMS 50L at NASA JSC. We followed analytical protocols that are well established in our laboratory [e.g., (27)]. Matrix regions in C0002 and A0040, one clast in C0002, and four clasts in A0040 were analyzed. The isotopic compositions of the samples were acquired by raster ion imaging using a 16-keV Cs^+ primary ion beam of ~0.9 pA and ~100 nm diameter. Before image acquisition, each analysis region was presputtered using a high beam current to remove the Pt coating, clean the sample surface, and ensure that secondary ion count rates reached a steady state. Negative secondary ions of the C and O isotopes, ^{28}Si, and either $^{24}Mg^{16}O$ or $^{27}Al^{16}O$ were collected simultaneously in electron multipliers. A mass resolving power of ~10,000 (CAMECA NanoSIMS definition) was achieved, and isobaric interferences were resolved. In particular, the ^{16}OH interference on ^{17}O was <1‰. A nuclear magnetic resonance probe was used to maintain the magnetic field stability to <10 ppm/10 hours; 20-μm fields of view were measured at an image size of 256 × 256 pixels. The dwell time was 3200 μs per pixel, and 60 image layers were acquired for each sample region. Automatic peak centering was conducted on ^{12}C and ^{16}O every 10 frames during the analyses to correct for any drift in the mass peaks. The other mass peaks were shifted accordingly. An electron flood gun was used to mitigate sample charging. To correct for instrumental mass fractionation, we measured San Carlos olivine to correct for O isotopes and USGS24 graphite for C isotopes. The graphite standard was on a separate mount and consisted of grains pressed into clean Au foil.

The interactive data language (IDL)–based L'image software, developed by L. Nittler, was used for data processing, and the following corrections were applied for each image pixel: deadtime correction of 44 ns, quasi-simultaneous arrival correction, and correction for shifts between image layers. Image layers are summed, and isotope ratio images are produced. Regions of interest are manually defined, and a grain was considered presolar if its isotopic composition differed from the surrounding material by >4σ. Likely phase identifications were based on the $^{28}Si/^{12}C$, $^{28}Si/^{16}O$, and $^{24}Mg^{16}O/^{16}O$ ratios; however, phases for representative grains were confirmed by TEM (see section below). Isotope ratio errors are based on counting statistical uncertainties and external reproducibility of standards. Ratios are reported as delta (δ) values, or per mil deviations (‰) from the reference value, and are calculated as δR (‰) = $[R_{sample}/R_{standard} - 1] \times 1000$, where R is the isotopic ratio of the sample and standard (table S1).

The area analyzed in each region for C and O isotopes was assessed on the basis of the NanoSIMS ^{16}O ion image with a 10% threshold applied. In other words, regions with counts below 10% of the maximum ^{16}O counts were excluded. Total analyzed areas for different samples and lithologies are reported in table S2. Presolar grain abundances were determined by dividing the total area covered by the presolar grains by the total area measured and are reported as ppm. Grain sizes are estimated from the NanoSIMS images. Errors in reported presolar grain abundances are based on the number of grains identified and use the confidence limits tables in (52). For regions where no presolar O-rich grains were identified, the 1σ upper limits on the abundances, given in table S2, were determined by using the average presolar O-rich grain size of 250 nm.

Some regions in clasts 1 and 2 and the matrix of C0002 and A0040 that were analyzed for C and O isotopes were remeasured for C, N, and Si isotopes to further characterize C-rich presolar grains (fig. S3) and to identify IAOM (table S3). Some of the C-rich presolar grains sputtered away during this subsequent analysis, and N and Si isotopic compositions for these grains could not be obtained. $^{12}C^-$, $^{13}C^-$, $^{12}C^{14}N^-$, $^{12}C^{15}N^-$, $^{28}Si^-$, $^{29}Si^-$, and $^{30}Si^-$ were measured simultaneously by ion imaging. Analytical protocols were similar to the previous measurement setup. USGS24 graphite was the reference material for the presolar grains for C isotopes. The KG17 kerogen standard was the reference material for N isotopes, and Si isotopic compositions were normalized to the average composition of the neighboring grains within the same imaged area. For organic matter, KG17 kerogen was the reference material for C and N isotopes. Organic matter was considered anomalous if its C and/or N isotopic ratios differed by at least 3σ from the average composition of the analyzed regions.

The concentration of IAOM was determined by dividing the area of anomalous organics by the total area analyzed. The area analyzed in each region was assessed on the basis of the ^{28}Si ion image, with a 10% threshold applied to the ^{28}Si counts. The total areas analyzed for C, N, and Si isotopes in clasts 1 and 2, the C0002 matrix, and the A0040 matrix were 1906, 4616, 5705, and 3401 μm², respectively. While grains with modest C anomalies ($\delta^{13}C$ ~ ±250‰) and low $^{28}Si/^{16}O$ ratios were identified during the C and O isotope mapping and are likely organic, these grains are not reported here because we do not have the corresponding N isotopic compositions to constrain their nature further (i.e., organic or presolar graphite). Only organic grains that were analyzed simultaneously for C and N isotopes are reported and included in the abundance calculation. This does not lead to an underestimate of the abundances of

IAOM because the areas analyzed for C and O isotopes were not included in the total area analyzed when calculating the abundances.

Phase identifications of presolar silicates, presolar SiC, presolar graphite, and organic matter were based on the $^{28}Si/^{12}C$, $^{28}Si/^{16}O$, and $^{24}Mg^{16}O/^{16}O$ ratios from NanoSIMS analysis. The relevant ratios for each grain are provided in tables S1 and S3. The TEM analysis of the presolar silicate and presolar SiC grains also assisted with phase identifications. A presolar grain was considered to be a silicate if its $^{28}Si/^{16}O$ and $^{24}Mg^{16}O/^{16}O$ ratios were equal to or greater than the average for the surrounding material, which is mainly composed of silicate grains. A grain was considered to be a SiC if a distinct ^{28}Si signal was observed to correlate with the isotopic anomaly or its $^{28}Si/^{12}C$ ratio was greater than 0.3. The relatively low $^{28}Si/^{12}C$ ratios of some grains that clearly showed ^{28}Si in the ion image, and thus were SiC, were due to contaminating signal from surrounding carbonaceous organic matter. Grains having $^{28}Si/^{12}C$ ratios lower than 0.3 were assigned as presolar graphite. Anomalous organic grains had a similar range of $^{28}Si/^{12}C$ ratios as presolar graphite, but their C and N isotopic signatures were distinct and aided in phase assignment. O, C, N, and Si isotopic ratios are reported relative to standard mean ocean water, Pee Dee Belemnite, air, and the Ryugu matrix, respectively.

FIB sample preparation

O- and C-rich presolar grains and an organic grain having N and C isotopic anomalies were extracted from the bulk sample and prepared for TEM analysis using FIB lift-out techniques. The FEI Quanta 3D-FEG 600 dual-beam FIB instrument at NASA JSC was used to produce thin (~100 nm) electron transparent cross sections of the grains and surrounding matrix. These sections were welded onto Cu grids for TEM analysis. Further description of the FIB sample preparation procedure can be found in (11).

TEM mineralogical and chemical analysis

The FIB sections were analyzed using a JEOL 2500SE 200 kV FE-STEM equipped with a JEOL 70 mm^2 SDD for EDX analyses. STEM images were collected in brightfield and darkfield modes. High-resolution (lattice fringe) images and selected-area electron diffraction (SAED) patterns were collected using a Gatan OneView camera. The compositional maps were acquired by rastering a 2-nm-diameter incident probe with a dwell time of 50 ms per pixel over a frame size of 200 × 256 pixels per frame. Multiple frames (200 to 500) were summed so that each pixel contains high-count EDX spectrum sufficient to provide better than 1% counting statistics to determine major elemental abundances (multiple pixels are summed to define a region of interest) and their spatial distributions. Quantitative analyses were obtained using the Cliff-Lorimer thin-film procedure, with experimental k-factors determined using well-characterized standards.

Supplementary Materials
This PDF file includes:
Figs. S1 to S10
Legends for tables S1 and S3
Table S2
References

Other Supplementary Material for this manuscript includes the following:
Tables S1 and S3

REFERENCES AND NOTES

1. T. Yokoyama, K. Nagashima, I. Nakai, E. D. Young, Y. Abe, J. Aléon, C. M. O.'. D. Alexander, S. Amari, Y. Amelin, K.-i. Bajo, M. Bizzarro, A. Bouvier, R. W. Carlson, M. Chaussidon, B.-G. Choi, N. Dauphas, A. M. Davis, T. Di Rocco, W. Fujiya, R. Fukai, I. Gautam, M. K. Haba, Y. Hibiya, H. Hidaka, H. Homma, P. Hoppe, G. R. Huss, K. Ichida, T. Ireland, A. Ishikawa, M. Ito, S. Itoh, N. Kawasaki, N. T. Kita, K. Kitajima, T. Kleine, S. Komatani, A. N. Krot, M.-C. Liu, Y. Masuda, K. D. McKeegan, M. Morita, K. Motomura, F. Moynier, A. Nguyen, L. Nittler, M. Onose, A. Pack, C. Park, L. Piani, L. Qin, S. S. Russell, N. Sakamoto, M. Schönbächler, L. Tafla, H. Tang, K. Terada, Y. Terada, T. Usui, S. Wada, M. Wadhwa, R. J. Walker, K. Yamashita, Q.-Z. Yin, S. Yoneda, H. Yui, A.-C. Zhang, H. C. Connolly, D. S. Lauretta, T. Nakamura, H. Naraoka, T. Noguchi, R. Okazaki, K. Sakamoto, H. Yabuta, M. Abe, M. Arakawa, A. Fujii, M. Hayakawa, N. Hirata, N. Hirata, R. Honda, C. Honda, S. Hosoda, Y.-i. Iijima, H. Ikeda, M. Ishiguro, Y. Ishihara, T. Iwata, K. Kawahara, S. Kikuchi, K. Kitazato, K. Matsumoto, M. Matsuoka, T. Michikami, Y. Mimasu, A. Miura, T. Morota, S. Nakazawa, N. Namiki, H. Noda, R. Noguchi, N. Ogawa, K. Ogawa, T. Okada, C. Okamoto, G. Ono, M. Ozaki, T. Saiki, N. Sakatani, H. Sawada, H. Senshu, Y. Shimaki, K. Shirai, S. Sugita, Y. Takei, H. Takeuchi, S. Tanaka, E. Tatsumi, F. Terui, Y. Tsuda, R. Tsukizaki, K. Wada, S.-i. Watanabe, M. Yamada, T. Yamada, Y. Yamamoto, H. Yano, Y. Yokota, K. Yoshihara, M. Yoshikawa, K. Yoshikawa, S. Furuya, K. Hatakeda, T. Hayashi, Y. Hitomi, K. Kumagai, A. Miyazaki, A. Nakato, M. Nishimura, H. Soejima, A. Suzuki, T. Yada, D. Yamamoto, K. Yogata, M. Yoshitake, S. Tachibana, H. Yurimoto, Samples returned from the asteroid Ryugu are similar to Ivuna-type carbonaceous meteorites. *Science* **379**, eabn7850 (2023).

2. E. Nakamura, K. Kobayashi, R. Tanaka, T. Kunihiro, H. Kitagawa, C. Potiszil, T. Ota, C. Sakaguchi, M. Yamanaka, D. M. Ratnayake, H. Tripathi, R. Kumar, M.-L. Avramescu, H. Tsuchida, Y. Yachi, H. Miura, M. Abe, R. Fukai, S. Furuya, K. Hatakeda, T. Hayashi, Y. Hitomi, K. Kumagai, A. Miyazaki, A. Nakato, M. Nishimura, T. Okada, H. Soejima, S. Sugita, A. Suzuki, T. Usui, T. Yada, D. Yamamoto, K. Yogata, M. Yoshitake, M. Arakawa, A. Fujii, M. Hayakawa, N. Hirata, N. Hirata, R. Honda, C. Honda, S. Hosoda, Y.-i. Iijima, H. Ikeda, M. Ishiguro, Y. Ishihara, T. Iwata, K. Kawahara, S. Kikuchi, K. Kitazato, K. Matsumoto, M. Matsuoka, T. Michikami, Y. Mimasu, A. Miura, T. Morota, S. Nakazawa, N. Namiki, H. Noda, R. Noguchi, N. Ogawa, K. Ogawa, C. Okamoto, G. Ono, M. Ozaki, T. Saiki, N. Sakatani, H. Sawada, H. Senshu, Y. Shimaki, K. Shirai, Y. Takei, H. Takeuchi, S. Tanaka, E. Tatsumi, F. Terui, R. Tsukizaki, K. Wada, M. Yamada, T. Yamada, Y. Yamamoto, H. Yano, Y. Yokota, K. Yoshihara, M. Yoshikawa, K. Yoshikawa, M. Fujimoto, S.-i. Watanabe, Y. Tsuda, On the origin and evolution of the asteroid Ryugu: A comprehensive geochemical perspective. *Proc. Jpn. Acad. B* **98**, 227–282 (2022).

3. T. Nakamura, M. Matsumoto, K. Amano, Y. Enokido, M. E. Zolensky, T. Mikouchi, H. Genda, S. Tanaka, M. Y. Zolotov, K. Kurosawa, S. Wakita, R. Hyodo, H. Nagano, D. Nakashima, Y. Takahashi, Y. Fujioka, M. Kikuiri, E. Kagawa, M. Matsuoka, A. J. Brearley, A. Tsuchiyama, M. Uesugi, J. Matsuno, Y. Kimura, M. Sato, R. E. Milliken, E. Tatsumi, S. Sugita, T. Hiroi, K. Kitazato, D. Brownlee, D. J. Joswiak, M. Takahashi, K. Ninomiya, T. Takahashi, T. Osawa, K. Terada, F. E. Brenker, B. J. Tkalcec, L. Vincze, R. Brunetto, A. Aléon-Toppani, Q. H. S. Chan, M. Roskosz, J. C. Viennet, P. Beck, E. E. Alp, T. Michikami, Y. Nagaashi, T. Tsuji, Y. Ina, J. Martinez, J. Han, A. Dolocan, R. J. Bodnar, M. Tanaka, H. Yoshida, K. Sugiyama, A. J. King, K. Fukushi, H. Suga, S. Yamashita, T. Kawai, K. Inoue, A. Nakato, T. Noguchi, F. Vilas, A. R. Hendrix, C. Jaramillo-Correa, D. L. Domingue, G. Dominguez, Z. Gainsforth, C. Engrand, J. Duprat, S. S. Russell, E. Bonato, C. Ma, T. Kawamoto, T. Wada, S. Watanabe, R. Endo, S. Enju, L. Riu, S. Rubino, P. Tack, S. Takeshita, Y. Takeichi, A. Takeuchi, A. Takigawa, D. Takir, T. Tanigaki, A. Taniguchi, K. Tsukamoto, T. Yagi, S. Yamada, K. Yamamoto, Y. Yamashita, M. Yasutake, K. Uesugi, I. Umegaki, I. Chiu, T. Ishizaki, S. Okumura, E. Palomba, C. Pilorget, S. M. Potin, A. Alasli, S. Anada, Y. Araki, N. Sakatani, C. Schultz, O. Sekizawa, S. D. Sitzman, K. Sugiura, M. Sun, E. Dartois, E. De Pauw, Z. Dionnet, Z. Djouadi, G. Falkenberg, R. Fujita, T. Fukuma, I. R. Gearba, K. Hagiya, M. Y. Hu, T. Kato, T. Kawamura, M. Kimura, M. K. Kubo, F. Langenhorst, C. Lantz, B. Lavina, M. Lindner, J. Zhao, B. Vekemans, D. Baklouti, B. Bazi, F. Borondics, S. Nagasawa, G. Nishiyama, K. Nitta, J. Mathurin, T. Matsumoto, I. Mitsukawa, H. Miura, A. Miyake, Y. Miyake, H. Yurimoto, R. Okazaki, H. Yabuta, H. Naraoka, K. Sakamoto, S. Tachibana, H. C. Connolly Jr., D. S. Lauretta, M. Yoshitake, M. Yoshikawa, K. Yoshikawa, Y. Yoshihara, Y. Yokota, K. Yogata, H. Yano, Y. Yamamoto, D. Yamamoto, M. Yamada, T. Yamada, T. Yada, K. Yada, T. Usui, R. Tsukizaki, F. Terui, H. Takeuchi, Y. Takei, A. Iwamae, H. Soejima, K. Shirai, Y. Shimaki, H. Senshu, H. Sawada, T. Saiki, M. Ozaki, G. Ono, T. Okada, N. Ogawa, K. Ogawa, R. Noguchi, H. Noda, M. Nishimura, N. Namiki, S. Nakazawa, T. Morota, A. Miyazaki, A. Miura, Y. Mimasu, K. Matsumoto, K. Kumagai, T. Kouyama, S. Kikuchi, K. Kawahara, S. Kameda, T. Iwata, Y. Ishihara, M. Ishiguro, H. Ikeda, S. Hosoda, R. Honda, C. Honda, Y. Hitomi, N. Hirata, N. Hirata, T. Hayashi, M. Hayakawa, K. Hatakeda, S. Furuya, R. Fukai, A. Fujii, Y. Cho, M. Arakawa, M. Abe, S. Watanabe, Y. Tsuda, Formation and evolution of carbonaceous asteroid Ryugu: Direct evidence from returned samples. *Science* **379**, eabn8671 (2023).

4. M. Ito, N. Tomioka, M. Uesugi, A. Yamaguchi, N. Shirai, T. Ohigashi, M.-C. Liu, R. C. Greenwood, M. Kimura, N. Imae, K. Uesugi, A. Nakato, K. Yogata, H. Yuzawa, Y. Kodama, A.

Tsuchiyama, M. Yasutake, R. Findlay, I. A. Franchi, J. A. Malley, K. A. McCain, N. Matsuda, K. D. McKeegan, K. Hirahara, A. Takeuchi, S. Sekimoto, I. Sakurai, I. Okada, Y. Karouji, M. Arakawa, A. Fujii, M. Fujimoto, M. Hayakawa, N. Hirata, N. Hirata, R. Honda, C. Honda, S. Hosoda, Y.-i. Iijima, H. Ikeda, M. Ishiguro, Y. Ishihara, T. Iwata, K. Kawahara, S. Kikuchi, K. Kitazato, K. Matsumoto, M. Matsuoka, T. Michikami, Y. Mimasu, A. Miura, O. Mori, T. Morota, S. Naka-zawa, N. Namiki, H. Noda, R. Noguchi, N. Ogawa, K. Ogawa, T. Okada, C. Okamoto, G. Ono, M. Ozaki, T. Saiki, N. Sakatani, H. Sawada, H. Senshu, Y. Shimaki, K. Shirai, S. Sugita, Y. Takei, H. Takeuchi, S. Tanaka, E. Tatsumi, F. Terui, R. Tsukizaki, K. Wada, K. Yamada, T. Yamada, Y. Yamamoto, H. Yano, Y. Yokota, K. Yoshihara, M. Yoshikawa, K. Yoshikawa, R. Fukai, S. Furuya, K. Hatakeda, T. Hayashi, Y. Hitomi, K. Kumagai, A. Miyazaki, M. Nishimura, H. Soejima, A. Iwamae, D. Yamamoto, M. Yoshitake, T. Yada, M. Abe, T. Usui, S.-i. Watanabe, Y. Tsuda, A pristine record of outer Solar System materials from asteroid Ryugu's returned sample. *Nat. Astron.* **6**, 1163–1171 (2022).

5. N. Kawasaki, K. Nagashima, N. Sakamoto, T. Matsumoto, K.-i. Bajo, S. Wada, Y. Igami, A. Miyake, T. Noguchi, D. Yamamoto, S. S. Russell, Y. Abe, J. Aléon, C. M. O.'. D. Alexander, S. Amari, Y. Amelin, M. Bizzarro, A. Bouvier, R. W. Carlson, M. Chaussidon, B.-G. Choi, N. Dauphas, A. M. Davis, T. Di Rocco, W. Fujiya, R. Fukai, I. Gautam, M. K. Haba, Y. Hibiya, H. Hidaka, H. Homma, P. Hoppe, G. R. Huss, K. Ichida, T. Iizuka, T. R. Ireland, A. Ishikawa, M. Ito, S. Itoh, N. T. Kita, K. Kitajima, T. Kleine, K. Komatani, A. N. Krot, M.-C. Liu, Y. Masuda, K. D. McKeegan, M. Morita, K. Motomura, F. Moynier, I. Nakai, A. Nguyen, L. Nittler, M. Onose, A. Pack, C. Park, L. Piani, L. Qin, M. Schönbächler, L. Tafla, H. Tang, K. Terada, Y. Terada, T. Usui, M. Wadhwa, R. J. Walker, K. Yamashita, Q.-Z. Yin, T. Yokoyama, S. Yoneda, E. D. Young, H. Yui, A.-C. Zhang, T. Nakamura, H. Naraoka, R. Okazaki, K. Sakamoto, H. Yabuta, M. Abe, A. Mi-yazaki, A. Nakato, M. Nishimura, T. Okada, T. Yada, K. Yogata, S. Nakazawa, T. Saiki, S. Tanaka, F. Terui, Y. Tsuda, S.-i. Watanabe, M. Yoshikawa, S. Tachibana, H. Yurimoto, Oxygen isotopes of anhydrous primary minerals show kinship between asteroid Ryugu and comet 81P/Wild2. *Sci. Adv.* **8**, eade2067 (2022).

6. G. L. F. Morin, Y. Marrocchi, J. Villeneuve, E. Jacquet, ^{16}O-rich anhydrous silicates in CI chondrites: Implications for the nature and dynamics of dust in the solar accretion disk. *Geochim. Cosmochim. Acta* **332**, 203–219 (2022).

7. E. Zinner, Presolar grains, in *Meteorites and Cosmochemical Processes*, A. M. Davis, Ed., vol. 1 of *Treatise on Geochemistry, 2nd Ed.*, H. D. Holland, K. K. Turekian, Exec. Eds. (Elsevier, 2014), vol. 1, pp. 181–213.

8. A. N. Nguyen, S. Messenger, Presolar history recorded in extraterrestrial materials. *Elements* **7**, 17–22 (2011).

9. C. Floss, P. Haenecour, Presolar silicate grains: Abundances, isotopic and elemental compositions, and the effects of secondary processing. *Geochem. J.* **50**, 3–25 (2016).

10. C. Davidson, H. Busemann, L. R. Nittler, C. M. O.'. D. Alexander, F.-R. Orthous-Daunay, I. A. Franchi, P. Hoppe, Abundances of presolar silicon carbide grains in primitive meteorites determined by NanoSIMS. *Geochim. Cosmochim. Acta* **139**, 248–266 (2014).

11. A. N. Nguyen, L. P. Keller, S. Messenger, Mineralogy of presolar silicate and oxide grains of diverse stellar origins. *Astrophys. J.* **818**, 51–67 (2016).

12. S. Messenger, Identification of molecular-cloud material in interplanetary dust particles. *Nature* **404**, 968–971 (2000).

13. H. Busemann, A. F. Young, C. M. O.'. D. Alexander, P. Hoppe, S. Mukhopadhyay, L. R. Nittler, Interstellar chemistry recorded in organic matter from primitive meteorites. *Science* **312**, 727–730 (2006).

14. J. Aléon, F. Robert, M. Chaussidon, B. Marty, Nitrogen isotopic composition of macromo-lecular organic matter in interplanetary dust particles. *Geochim. Cosmochim. Acta* **67**, 3773–3783 (2003).

15. C. M. O.'. D. Alexander, G. D. Cody, B. T. De Gregorio, L. R. Nittler, R. M. Stroud, The nature, origin and modification of insoluble organic matter in chondrites, the major source of Earth's C and N. *Geochemistry* **77**, 227–256 (2017).

16. S. B. Charnley, S. D. Rodgers, The end of interstellar chemistry as the origin of nitrogen in comets and meteorites. *Astrophys. J.* **569**, L133–L137 (2002).

17. S. D. Rodgers, S. B. Charnley, Nitrogen isotopic fractionation of interstellar nitriles. *Astro-phys. J.* **689**, 1448–1455 (2008).

18. C. Floss, F. J. Stadermann, High abundances of circumstellar and interstellar C-anomalous phases in the primitive CR3 chondrites QUE 99177 and MET 00426. *Astrophys. J.* **697**, 1242–1255 (2009).

19. L. R. Nittler, C. M. O.'. D. Alexander, J. Davidson, M. E. I. Riebe, R. M. Stroud, J. Wang, High abundances of presolar grains and ^{15}N-rich organic matter in CO3.0 chondrite Dominion Range 08006. *Geochim. Cosmochim. Acta* **226**, 107–131 (2018).

20. C. Floss, F. J. Stadermann, J. Bradley, Z. R. Dai, S. Bajt, G. Graham, Carbon and nitrogen isotopic anomalies in an anhydrous interplanetary dust particle. *Science* **303**, 1355–1358 (2004).

21. H. Busemann, A. N. Nguyen, G. D. Cody, P. Hoppe, A. L. D. Kilcoyne, R. M. Stroud, T. J. Zega, L. R. Nittler, Ultra-primitive interplanetary dust particles from the comet 26P/Grigg-Skjellerup dust stream collection. *Earth Planet. Sci. Lett.* **288**, 44–57 (2009).

22. J. Barosch, L. R. Nittler, J. Wang, C. M. O.'. D. Alexander, B. T. De Gregorio, C. Engrand, Y. Kebukawa, K. Nagashima, R. M. Stroud, H. Yabuta, Y. Abe, J. Aléon, S. Amari, Y. Amelin, K.-i. Bajo, L. Bejach, M. Bizzarro, L. Bonal, A. Bouvier, R. W. Carlson, M. Chaussidon, B.-G. Choi, G. D. Cody, E. Dartois, N. Dauphas, A. M. Davis, A. Dazzi, A. Deniset-Besseau, T. Di Rocco, J. Duprat, W. Fujiya, R. Fukai, I. Gautam, M. K. Haba, M. Hashiguchi, Y. Hibiya, H. Hidaka, H. Homma, P. Hoppe, G. R. Huss, K. Ichida, T. Iizuka, T. R. Ireland, A. Ishikawa, M. Ito, S. Itoh, K. Kamide, N. Kawasaki, A. L. D. Kilcoyne, N. T. Kita, K. Kitajima, T. Kleine, S. Komatani, M. Komatsu, A. N. Krot, M.-C. Liu, Z. Martins, Y. Masuda, J. Mathurin, K. D. McKeegan, G. Montagnac, M. Morita, S. Mostefaoui, K. Motomura, F. Moynier, I. Nakai, A. N. Nguyen, T. Ohigashi, T. Okumura, M. Onose, A. Pack, C. Park, L. Piani, L. Qin, E. Quirico, L. Remusat, S. S. Russell, N. Sakamoto, S. A. Sandford, M. Schönbächler, M. Shigenaka, H. Suga, L. Tafla, Y. Takahashi, Y. Takeichi, T. Tamenori, H. Tang, K. Terada, Y. Terada, T. Usui, M. Verdier-Paoletti, S. Wada, M. Wadhwa, D. Wakabayashi, R. J. Walker, K. Yamashita, S. Yamashita, Q.-Z. Yin, T. Yokoyama, S. Yoneda, E. D. Young, H. Yui, A.-C. Zhang, M. Abe, A. Miyazaki, A. Nakato, S. Nakazawa, M. Nishimura, T. Okada, T. Saiki, S. Tanaka, F. Terui, Y. Tsuda, S.-i. Watanabe, T. Yada, K. Yogata, M. Yoshikawa, T. Nakamura, H. Naraoka, T. Noguchi, R. Okazaki, K. Saka-moto, S. Tachibana, H. Yurimoto, Presolar stardust in asteroid Ryugu. *Astrophys. J. Lett.* **935**, L3 (2022).

23. N. M. Abreu, A. J. Brearley, Early solar system processes recorded in the matrices of two highly pristine CR3 carbonaceous chondrites, MET 00426 and QUE 99177. *Geochim. Cos-mochim. Acta* **74**, 1146–1171 (2010).

24. C. Le Guillou, H. G. Changela, A. J. Brearley, Widespread oxidized and hydrated amorphous silicates in CR chondrites matrices: Implications for alteration conditions and H2 degassing of asteroids. *Earth Planet. Sci. Lett.* **420**, 162–173 (2015).

25. P. Haenecour, C. Floss, T. J. Zega, T. K. Croat, A. Wang, B. L. Jolliff, P. Carpenter, Presolar silicates in the matrix and fine-grained rims around chondrules in primitive CO3.0 chon-drites: Evidence for pre-accretionary aqueous alteration of the rims in the solar nebula. *Geochim. Cosmochim. Acta* **221**, 379–405 (2018).

26. C. Floss, F. J. Stadermann, A. T. Kearsley, M. J. Burchell, W. J. Ong, The abundance of presolar grains in comet 81P/Wild 2. *Astrophys. J.* **763**, 140–150 (2013).

27. A. N. Nguyen, K. Nakamura-Messenger, L. P. Keller, S. Messenger, Diverse assemblage of presolar and solar system materials in anhydrous interplanetary dust particles: Coordinated NanoSIMS and TEM analyses. *Geochim. Cosmochim. Acta* **336**, 131–149 (2022).

28. C. Floss, F. J. Stadermann, J. P. Bradley, Z. R. Dai, S. Bajt, G. Graham, A. S. Lea, Identification of isotopically primitive interplanetary dust particles: A NanoSIMS isotopic imaging study. *Geochim. Cosmochim. Acta* **70**, 2371–2399 (2006).

29. C. M. O.'. D. Alexander, L. R. Nittler, J. Davidson, F. J. Ciesla, Measuring the level of inter-stellar inheritance in the solar protoplanetary disk. *Meteorit. Planet. Sci.* **52**, 1797–1821 (2017).

30. L. R. Nittler, R. M. Stroud, J. M. Trigo-Rodríguez, B. T. De Gregorio, C. M. O.'. D. Alexander, J. Davidson, C. E. Moyano-Cambero, S. Tanbakouei, A cometary building block in a primitive asteroidal meteorite. *Nat. Astron.* **3**, 659–666 (2019).

31. T. Yada, C. Floss, F. J. Stadermann, E. Zinner, T. Nakamura, T. Noguchi, A. S. Lea, Stardust in Antarctic micrometeorites. *Meteorit. Planet. Sci.* **43**, 1287–1298 (2008).

32. G. R. Huss, A. P. Meshik, J. B. Smith, C. M. Hohenberg, Presolar diamond, silicon carbide, and graphite in carbonaceous chondrites: Implications for thermal processing in the solar nebula. *Geochim. Cosmochim. Acta* **67**, 4823–4848 (2003).

33. G. R. Huss, R. S. Lewis, Presolar diamond, SiC, and graphite in primitive chondrites: Abundances as a function of meteorite class and petrologic type. *Geochim. Cosmochim. Acta* **59**, 115–160 (1995).

34. J. Davidson, H. Busemann, I. A. Franchi, A NanoSIMS and Raman spectroscopic comparison of interplanetary dust particles from comet Grigg-Skjellerup and non-Grigg Skjellerup collections. *Meteorit. Planet. Sci.* **47**, 1748–1771 (2012).

35. F. J. Stadermann, C. Floss, B. Wopenka, Circumstellar aluminum oxide and silicon carbide in interplanetary dust particles. *Geochim. Cosmochim. Acta* **70**, 6168–6179 (2006).

36. J. Leitner, C. Vollmer, P. Hoppe, J. Zipfel, Characterization of presolar material in the CR chondrite Northwest Africa 852. *Astrophys. J.* **745**, 38 (2012).

37. X. Zhao, C. Floss, Y. Lin, M. Bose, Stardust investigation into the CR chondrite Grove Mountain 021710. *Astrophys. J.* **769**, 49 (2013).

38. P. H. Warren, Stable-isotopic anomalies and the accretionary assemblage of the Earth and Mars: A subordinate role for carbonaceous chondrites. *Earth Planet. Sci. Lett.* **311**, 93–100 (2011).

39. C. Burkhardt, T. Kleine, F. Oberli, A. Pack, B. Bourdon, R. Wieler, Molybdenum isotope anomalies in meteorites: Constraints on solar nebula evolution and origin of the Earth. *Earth Planet. Sci. Lett.* **312**, 390–400 (2011).

40. K. L. Thomas, G. E. Blanford, L. P. Keller, W. Klöck, D. S. McKay, Carbon abundance and silicate mineralogy of anhydrous interplanetary dust particles. *Geochim. Cosmochim. Acta* **57**, 1551–1566 (1993).

41. E. Dartois, C. Engrand, R. Brunetto, J. Duprat, T. Pino, E. Quirico, L. Remusat, N. Bardin, G. Briani, S. Mostefaoui, G. Morinaud, B. Crane, N. Szwec, L. Delauche, F. Jamme, C. Sandt, P.

Dumas, UltraCarbonaceous Antarctic micrometeorites, probing the Solar System beyond the nitrogen snow-line. *Icarus* **224**, 243–252 (2013).

42. S. A. Sandford, J. Aléon, C. M. O.'. D. Alexander, T. Araki, S. Bajt, G. A. Baratta, J. Borg, J. P. Bradley, D. E. Brownlee, J. R. Brucato, M. J. Burchell, H. Busemann, A. Butterworth, S. J. Clemett, G. Cody, L. Colangeli, G. Cooper, L. D'Hendecourt, Z. Djouadi, J. P. Dworkin, G. Ferrini, H. Fleckenstein, G. J. Flynn, I. A. Franchi, M. Fries, M. K. Gilles, D. P. Glavin, M. Gou-nelle, F. Grossemy, C. Jacobsen, L. P. Keller, A. L. D. Kilcoyne, J. Leitner, G. Matrajt, A. Meibom, V. Mennella, S. Mostefaoui, L. R. Nittler, M. E. Palumbo, D. A. Papanastassiou, F. Robert, A. Rotundi, C. J. Snead, M. K. Spencer, F. J. Stadermann, A. Steele, T. Stephan, P. Tsou, T. Tyliszczak, A. J. Westphal, S. Wirick, B. Wopenka, H. Yabuta, R. N. Zare, M. E. Zolensky, Organics captured from comet 81P/Wild 2 by the Stardust spacecraft. *Science* **314**, 1720–1724 (2006).

43. C. Floss, C. Le Guillou, A. Brearley, Coordinated NanoSIMS and FIB-TEM analyses of organic matter and associated matrix materials in CR3 chondrites. *Geochim. Cosmochim. Acta* **139**, 1–25 (2014).

44. G. Matrajt, S. Messenger, D. Brownlee, D. Joswiak, Diverse forms of primordial organic matter identified in interplanetary dust particles. *Meteorit. Planet. Sci.* **47**, 525–549 (2012).

45. K. D. McKeegan, J. Aleon, J. Bradley, D. Brownlee, H. Busemann, A. Butterworth, M. Chaussidon, S. Fallon, C. Floss, J. Gilmour, M. Gounelle, G. Graham, Y. Guan, P. R. Heck, P. Hoppe, I. D. Hutcheon, J. Huth, H. Ishii, M. Ito, S. B. Jacobsen, A. Kearsley, L. A. Leshin, M.-C. Liu, I. Lyon, K. Marhas, B. Marty, G. Matrajt, A. Meibom, S. Messenger, S. Mostefaoui, S. Mukhopadhyay, K. Nakamura-Messenger, L. Nittler, R. Palma, R. O. Pepin, D. A. Papanas-tassiou, F. Robert, D. Schlutter, C. J. Snead, F. J. Stadermann, R. Stroud, P. Tsou, A. Westphal, E. D. Young, K. Ziegler, L. Zimmermann, E. Zinner, Isotopic compositions of cometary matter returned by Stardust. *Science* **314**, 1724–1728 (2006).

46. B. T. De Gregorio, R. M. Stroud, L. R. Nittler, C. M. O.'. D. Alexander, A. L. D. Kilcoyne, T. J. Zega, Isotopic anomalies in organic nanoglobules from Comet 81P/Wild 2: Comparison to Murchison nanoglobules and isotopic anomalies induced in terrestrial organics by electron irradiation. *Geochim. Cosmochim. Acta* **74**, 4454–4470 (2010).

47. C. M. O.'. D. Alexander, M. Fogel, H. Yabuta, G. D. Cody, The origin and evolution of chondrites recorded in the elemental and isotopic compositions of their macromolecular organic matter. *Geochem. Cosmochim. Acta* **71**, 4380–4403 (2007).

48. E. S. Wirström, S. B. Charnley, M. A. Cordiner, S. N. Milam, Isotopic anomalies in primitive solar system matter: Spin-state-dependent fractionation of nitrogen and deuterium in in-terstellar clouds. *Astrophys. J. Lett.* **757**, L11 (2012).

49. W. D. Langer, T. E. Graedel, Ion-molecule chemistry of dense interstellar clouds: Nitrogen-, oxygen-, and carbon-bearing molecule abundances and isotopic ratios. *Astrophys. J.* **69**, 241–269 (1989).

50. W. D. Langer, T. E. Graedel, M. A. Frerking, P. B. Armentrout, Carbon and oxygen isotope fractionation in dense interstellar clouds. *Astrophys. J.* **277**, 581–604 (1984).

51. L. R. Nittler, C. M. O.'. D. Alexander, A. Patzer, M. J. Verdier-Paoletti, Presolar stardust in highly pristine CM chondrites Asuka 12169 and Asuka 12236. *Meteorit. Planet. Sci.* **56**, 260–276 (2021).

52. N. Gehrels, Confidence limits for small numbers of events in astrophysical data. *Astrophys. J.* **303**, 336–346 (1986).

53. T. Stephan, M. Bose, A. Boujibar, A. M. Davis, F. Gyngard, P. Hoppe, K. M. Hynes, N. Liu, L. R. Nittler, R. C. Ogliore, R. Trappitsch, The presolar grain database reloaded—Silicon carbide, paper presented at the 51st Lunar and Planetary Science Conference, The Woodlands, TX, 16 to 20 March 2020.

54. K. M. Hynes, F. Gyngard, The presolar grain database: http://presolar.wustl.edu/~pgd. *Lunar Planet. Sci.* **XL**, Abstract # 1198 (2009).

Abundant presolar grains and primordial organics preserved in carbon-rich exogenous clasts in asteroid Ryugu

Ann. N. Nguyen, Prajkta Mane, Lindsay P. Keller, Laurette Piani, Yoshinari Abe, Jrme Alon, Conel M. O'D. Alexander, Sachiko Amari, Yuri Amelin, Ken-ichi Bajo, Martin Bizzarro, Audrey Bouvier, Richard W. Carlson, Marc Chaussidon, Byeon-Gak Choi, Nicolas Dauphas, Andrew M. Davis, Tommaso Di Rocco, Wataru Fujiya, Ryota Fukai, Ikshu Gautam, Makiko K. Haba, Yuki Hibiya, Hiroshi Hidaka, Hisashi Homma, Peter Hoppe, Gary R. Huss, Kiyohiro Ichida, Tsuyoshi Iizuka, Trevor R. Ireland, Akira Ishikawa, Shoichi Itoh, Noriyuki Kawasaki, Noriko T. Kita, Kouki Kitajima, Thorsten Kleine, Shintaro Komatani, Alexander N. Krot, Ming-Chang Liu, Yuki Masuda, Kevin D. McKeegan, Mayu Morita, Kazuko Motomura, Frdric Moynier, Izumi Nakai, Kazuhide Nagashima, David Nesvorn, Larry Nittler, Morihiko Onose, Andreas Pack, Changkun Park, Liping Qin, Sara S. Russell, Naoya Sakamoto, Maria Schnbchler, Lauren Tafla, Haolan Tang, Kentaro Terada, Yasuko Terada, Tomohiro Usui, Sohei Wada, Meenakshi Wadhwa, Richard J. Walker, Katsuyuki Yamashita, Qing-Zhu Yin, Tetsuya Yokoyama, Shigekazu Yoneda, Edward D. Young, Hiroharu Yui, Ai-Cheng Zhang, Tomoki Nakamura, Hiroshi Naraoka, Takaaki Noguchi, Ryuji Okazaki, Kanako Sakamoto, Hikaru Yabuta, Masanao Abe, Akiko Miyazaki, Aiko Nakato, Masahiro Nishimura, Tatsuaki Okada, Toru Yada, Kasumi Yogata, Satoru Nakazawa, Takanao Saiki, Satoshi Tanaka, Fuyuto Terui, Yuichi Tsuda, Sei-ichiro Watanabe, Makoto Yoshikawa, Shogo Tachibana, and Hisayoshi Yurimoto

View the article online
https://www.science.org/doi/10.1126/sciadv.adh1003
Permissions
https://www.science.org/help/reprints-and-permissions

Use of this article is subject to the Terms of service